DOI: 10.1002/ejoc.200600807

Conformational and Structural Analysis of a *ter*-Cyclopentane Scaffold for Molecular Recognition

Peter C. Gareiss,[a] Prakash B. Palde,[a] Robert D. Hubbard,[b][‡] and Benjamin L. Miller*[a,c,d]

Keywords: Molecular modeling / Molecular recognition / Conformational analysis

Well-defined oligomers of cycloalkanes comprise a relatively unstudied class of organic compounds, and may have general utility in the development of receptors for biologically relevant molecules. We have investigated the solution structure of a *ter*-cyclopentane member of this class by molecular modeling and by NMR spectroscopy. We find that the molecular ensembles derived from conformational searches incorporating NMR-derived restraints are in excellent qualitative agreement with unrestrained molecular mechanics conformation searches. The *ter*-cyclopentane scaffold adopts an extended rigid conformation, with inter-ring torsion angles preferentially at 180°. These experiments demonstrate that conformational hypotheses developed in the course of designing *ter*-cyclopentane scaffolds for lipid A recognition are accurate, and furthermore provide support to the broader use of this class of compounds as scaffolds in molecular recognition.

Introduction

Organic chemistry has a rich tradition of employing conformational restraint in the design and synthesis of novel molecules. From early observations of the conformational bias of substituted cyclohexanes,[1] to more recent efforts in "conformational design" by Still,[2] Hoffmann,[3,4] and others,[5–7] consideration of conformational bias allows for the generation of complex organic structures with predictable three-dimensional solution structures. In turn, this conformational predictability can be a strategy-level design element in the development of molecules targeting a specific biological function.

As part of a general program directed towards the identification of novel receptors for carbohydrates and carbohydrate derivatives, we initiated a study of the synthesis and properties of substituted, stereoregular oligocycloalkanes (**1**). Such compounds seemed interesting at the outset for several reasons. First, relatively few examples of this structural class have been described in the literature.[8,9] The oligocyclopropane natural products FR-900848 (**2**)[10] and U-106305 (**3**)[11] (versions of **1** in which $l = m = n = 0$) are essentially the only naturally occurring members of this group of compounds incorporating more than two rings, and their interesting biological activity and novel structure have driven an extensive effort in the synthetic community.[12] Second, oligocycloalkanes appeared to provide a new set of structural motifs for conformational design. We anticipated that other oligocycloalkanes would have intrinsic interest as novel materials, requiring development of new synthetic methodology. Ultimately, oligocycloalkanes were envisioned to serve as potential scaffolds for the construction of new molecular recognition systems (Figure 1).

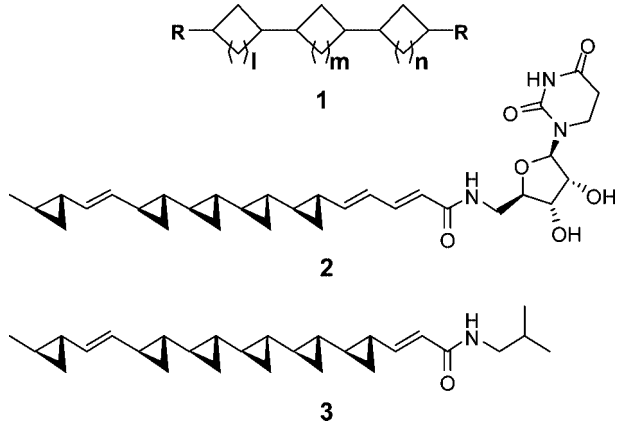

Figure 1. Examples of stereoregular oligocycloalkanes.

As we have reported previously,[13] our study of the synthesis and properties of oligocycloalkanes began with the design and synthesis of the *ter*-cyclopentane derivative **4**.

[a] Department of Biochemistry and Biophysics, University of Rochester,
Rochester, New York, USA
[b] Department of Chemistry, University of Rochester,
Rochester, New York, USA
[c] Department of Dermatology, University of Rochester,
Rochester, New York, USA
[d] The Center for Future Health, University of Rochester,
Rochester, New York, USA
[‡] Current address: Abbott Laboratories, Abbott Park, Illinois, USA

Supporting information for this article is available on the WWW under http://www.eurjoc.org or from the author.

This molecule binds lipid A, the component of bacterial lipopolysaccharide believed to be responsible for most cases of Gram-(–) bacterial sepsis,[14] with an affinity rivaling that of lipid A-binding natural products such as the topical antibiotic polymyxin B.[15] In addition, compound **4** proved useful as the recognition component of a label-free optical sensor for Gram-(–) bacteria.[16] Our design of **4** as a lipid A receptor was primarily based on molecular mechanics calculations. To more clearly understand the molecular recognition process, and lend information to the future development of new receptors for lipid A and other glycoconjugates, it was necessary to experimentally validate the computational models. Herein, we present the conformational analysis, synthesis, and solution NMR structures of the tetra-alcohol *ter*-cyclopentane derivative **5** (Figure 2). Gratifyingly, we demonstrate a strong correlation between conformational biases predicted by molecular mechanics and experimentally determined solution structures for *ter*-cyclopentanes.

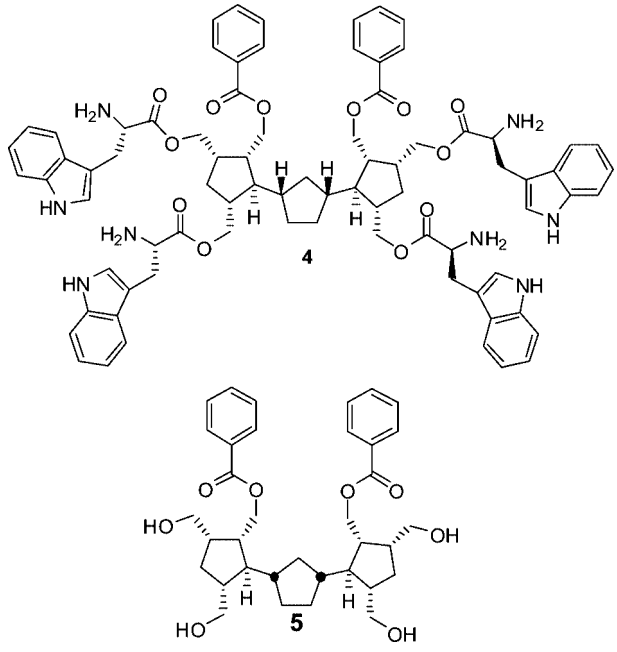

Figure 2. Structure of the lipid A binding tetra-tryptophan *ter*-cyclopentane derivative **4**, and the tetra-alcohol *ter*-cyclopentane synthetic precursor, **5**.

Our initial molecular modeling efforts focused on simple dihedral angle drives in order to map out the conformational preferences of oligocyclopentanes. Because parameterization varies from force field to force field, this also afforded us an opportunity to examine whether there were any force field-based differences in the potential energy surface. To provide a benchmark for comparison, we began with the well-studied compound 2,3-dimethylbutane. One might predict based on a simple "back of the envelope" drawing of Newman projections that the *anti* structure would be lower in energy than the two degenerate *gauche* conformers. However, both high-level computational and experimental studies have indicated that these conformers are essentially isoenergetic.[17–21] This is presumably because steric repulsion by the methyl groups in the *anti* conformer destabilizes this structure. Dihedral angle drive calculations employing a number of different force fields implemented in the Maestro/Macromodel molecular mechanics package[22] indicate that all are able to reproduce this behavior both in the gas phase and when continuum solvation terms (GB/SA water or chloroform)[23] are included in the calculation (data not shown).

Next, we calculated the energies for the *anti* and *gauche* conformers of 1-(cyclopentyl)cyclopentane, starting from an envelope–envelope[24–26] conformer in which each cyclopentyl is an equatorial substituent of the other. We anticipated that the geometric constraints of the cyclopentane rings would force inter-ring bond angles to open sufficiently to allow the "intuitive ranking" of conformers to hold true. Indeed, this is what we observed for all force fields in both the gas phase and GB/SA solvent (water or $CHCl_3$) (Table 1). It is unsurprising that Amber* and OPLS* produce ΔE(*gauche* – *anti*) slightly different from the other force fields, because the parameterization of these force

Table 1. Calculated steric energies (kcal/mol) for *gauche* and *anti* conformers of 1-(cyclopentyl)cyclopentane with various force fields and gas phase or GB/SA solvent (water or $CHCl_3$).

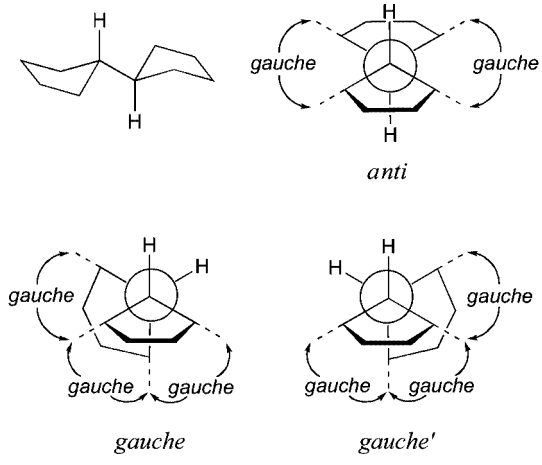

	Force Field	*gauche*	*anti*	ΔE
Gas Phase				
	MM2*	24.1	22.2	1.9
	MM3*	38.4	36.5	1.9
	Amber*	21.1	19.6	1.5
	OPLS*	18.8	16.7	2.1
	MMFFs*	17.4	16.7	1.7
GB/SA $CHCl_3$				
	MM2*	18.2	16.7	1.5
	MM3*	32.5	30.5	2.0
	Amber*	15.2	13.6	1.5
	OPLS*	12.8	10.7	2.1
	MMFFs*	11.5	9.7	1.8
GB/SA H_2O				
	MM2*	26.5	25.1	1.4
	MM3*	40.8	38.9	1.9
	Amber*	22.9	21.3	1.6
	OPLS*	21.1	19.0	2.1
	MMFFs*	19.7	18.0	1.7

fields is primarily biopolymer-directed. As with all molecular mechanics calculations, it is the differences in energy between conformations that are important and not their absolute values.

Introduction of a third cyclopentane ring at the 3-position reduces the level of symmetry in the molecule [vs. 1-(cyclopentyl)cyclopentane], and we were interested in determining the structural impact of this, as well as additional substitution. We concentrated on the *meso* isomer (or 1,3-*cis*), primarily for reasons of synthetic accessibility, but also because it appeared more suitable as a scaffold for the development of receptor molecules. The all-envelope conformation was chosen for dihedral angle analysis of *cis*-(1,3-dicyclopentyl)cyclopentane (**6**), with cyclopentyl substituents of the central cyclopentane ring in **6** placed pseudo-equatorially (Figure 3). For the hexamethyl-substituted *ter*-cyclopentane **7**, methyl-substituted rings twist out of the envelope conformation in order to minimize steric repulsion. Results of the two dihedral angle drive calculations are shown in Figure 4. In each case, the lowest energy conformer was found to be that with both inter-ring torsion angles *anti*, with a 1.9 kcal/mol difference in energy separating the lowest energy conformer from the next-lowest (*gauche*) for **6**. Barriers between neighboring *gauche* conformers for **6** were found to be on the order of 5.4 kcal/mol. Interestingly, although the potential energy surface for **7** is similar to that calculated for **6**, it is not identical. Rather, a slight asymmetry is observed, with one *anti*,-*gauche* conformation predicted to lie just 0.2 kcal/mol in energy higher than the global energy minimum (*anti*,*anti*). Barriers to conformational interconversion for **7** are also asymmetric, varying from 4 to 6.3 kcal/mol. While the observed asymmetry may be in part an artifact of the way the dihedral angle drive calculation is run (i.e., no pseudorotation of cyclopentane rings is allowed, and thus the calculation yields a somewhat unrealistic view of the potential energy surface), the non-symmetrical substitution of the cyclopentane rings is almost certainly a contributor as well. Taken together, these data suggested that although *ter*-cyclopentane scaffolds have some conformational flexibility, there is a significant energetic preference for the *anti*,*anti* conformer. Substitution of the core scaffold changes the potential energy surface somewhat, allowing the *gauche*,*anti* conformer to nearly match the *anti*,*anti* conformer. Of course, we anticipate that further substitution of the scaffold for utility as a functional receptor could potentially alter the conformational ensemble, either enhancing or reducing the degree to which the all-*anti* conformer is favored.

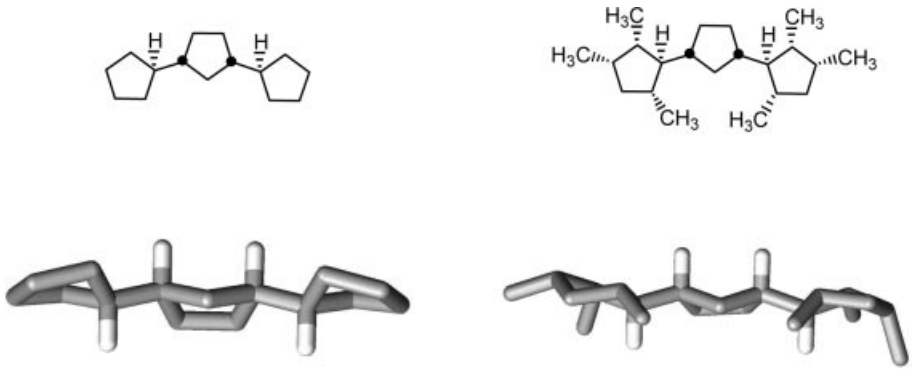

Figure 3. Starting conformations for *ter*-cyclopentane (**6**, left) and hexamethyl *ter*-cyclopentane (**7**, right) dihedral angle drives. Only protons flanking the critical torsion angles are shown.

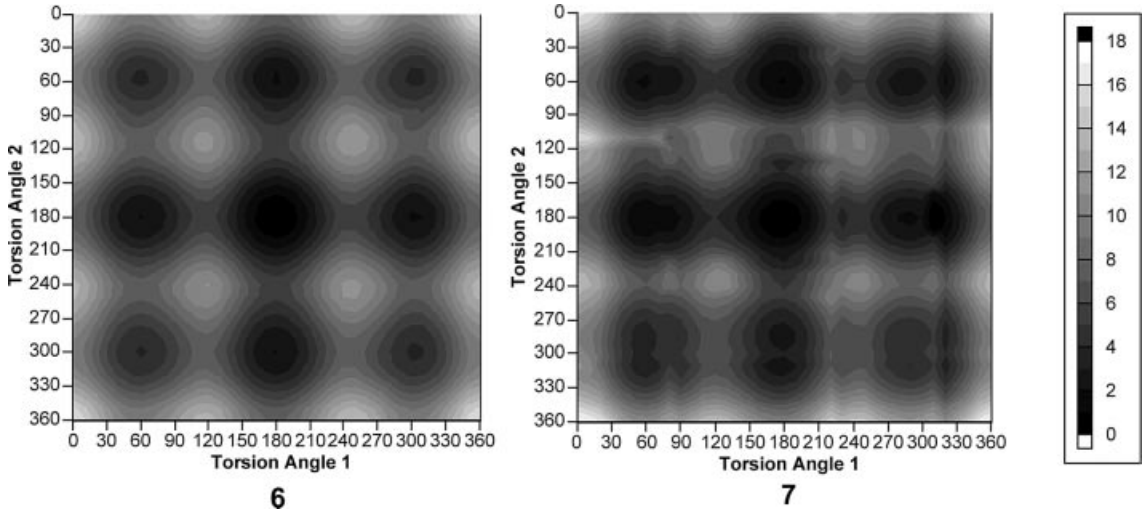

Figure 4. Dihedral angle drive for **6** and **7**. Legend indicates relative energy in kcal/mol.

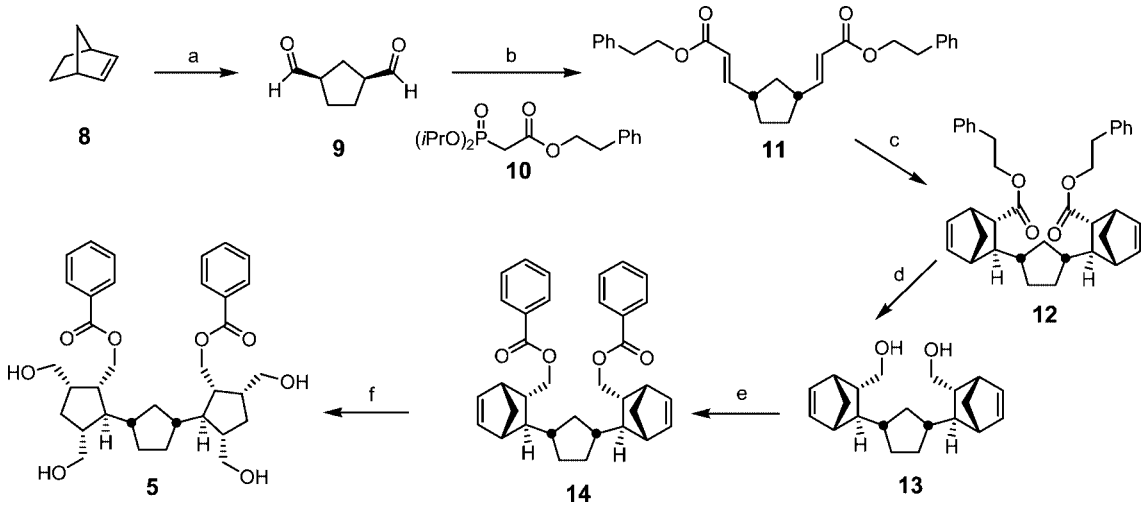

Scheme 1. (a) $KMnO_4$ on $CuSO_4$, CH_2Cl_2, room temp., 12 h; (b) KO*t*Bu, THF, 0 °C to room temp. 2 h, then –78 °C, **10**, 10 h (61% over 2 steps); (c) $(CH_3)_3Al$ (0.05 equiv.), $AlCl_3$ (0.5 equiv.), cyclopentadiene (10 equiv.), CH_2Cl_2, 4 °C, 18 h (15%); (d) $LiAlH_4$ (6 equiv.), THF, room temp., 24 h (51%); (e) benzoyl chloride (3.6 equiv.), Et_3N (4 equiv.), CH_2Cl_2, room temp., 3 h (35%); (f) O_3, CH_2Cl_2/CH_3OH (1:1), –78 °C, 15 min., then $NaBH_4$ (20 equiv.), 4 h (89%).

Synthesis

The optimized route currently used to synthesize the *ter*-cyclopentane scaffolds is shown in Scheme 1. The synthesis of **5** begins with oxidative cleavage of norbornene (**8**) to afford cyclopentane-1,3-dialdehyde (**9**). While the synthesis of **9** from **8** has been well precedented, the reported yields were low (40–50%) and in our hands were not amenable to large-scale synthesis (>3 g). After surveying a broad range of oxidants (including ozonolysis, wet permanganate and alumina,[27] and a two-step Sharpless dihydroxylation[28]/oxidative cleavage procedure), we found a procedure employing $KMnO_4$ adsorbed on copper sulfate[29] to be reproducibly high-yielding (essentially quantitative) and scalable.

Conversion of the dialdehyde **9** to the bis(α,β-unsaturated ester) **11** was accomplished by a bidirectional Horner–Wadsworth–Emmons reaction employing the phosphonate **10**.[30] By analogy to previous observations by Kishi,[31] we chose diisopropyl phosphonate in order to improve the *E*:*Z* selectivity, while the phenethyl ester was solely selected to simplify chromatographic detection of the product. To a solution of the phosphonate **10** in THF was added potassium *tert*-butoxide. Cannulation of the yellow anion into a THF solution of the di-aldehyde **9** at –78 °C, followed by warming the reaction to 4 °C, and stirring at this temperature for 18 h afforded the desired product **11** in 61% yield, and *E,E*:*E,Z* selectivity of at least 20:1.

With **11** in hand, we were ready to perform the bi-directional Diels–Alder reaction, using a Lewis acid catalyst we had previously examined in the context of a "unidirectional" model system.[31] The bis-dienophile **11** was dissolved into CH_2Cl_2, and cooled to 0 °C. The solution was treated with Me_3Al (0.05 equiv.) and $AlCl_3$ (0.5 equiv.) at 0 °C. Cyclopentadiene (10 equiv.) was added to the reaction; the reaction was then warmed to 4 °C and stirred for 18 h. After standard work-up and flash chromatography, a mixture of the *endo–endo* convex–convex and convex–concave/concave–convex diastereomers of the cycloadduct **12** was obtained in 70% yield. Final purification of the convex–convex diastereomer was accomplished in 15% yield by reverse phase (C_{18}) preparatory HPLC.

Reduction of diastereomerically pure **12** with $LiAlH_4$ in THF followed by double benzoylation provided **14** in moderate yield (18% over the two steps). Subsequent ozonolysis in a 1:1 $MeOH/CH_2Cl_2$ solution at –78 °C and reductive workup with $NaBH_4$ (–78 °C to room temperature) cleanly provided tetrol **5** as a faint yellow oil in 89% yield. Our choice of benzoyl derivatization prior to ozonolysis was governed in part by synthetic accessibility; previous attempts at bis-silylation were unsuccessful.

NMR Spectra of Tetra-Alcohol 5 in CD_3OD

With the tetra-alcohol **5** in hand, we were ready to begin solution NMR analysis. The one-dimensional ^1H and ^{13}C spectra, while too complex by themselves to allow full assignment, provided useful information about the structure of **5** in CD_3OD at room temperature. First, integration of peaks revealed an upfield multiplet corresponding to a single proton. By simple geometry, this must correspond to one of the diastereotopic protons on the central ring, at the *meso* plane of symmetry. This observation was crucial to assigning the rest of the protons on the molecule. Completion of the assignment of the *ter*-cyclopentane ring core of **5** was accomplished following acquisition of a full suite of ^1H-^1H (DQF-COSY and NOESY) and ^1H-^{13}C (HSQC) spectra (Table 2). Analysis of the DQF-COSY experiment allowed for extraction of a critical torsional angle restraint: the crosspeak connecting H^1, $H^{1''}$ and $H^{1'}$, $H^{3'}$ showed a coupling constant of 14 Hz (at an acquired digital resolution of 2.9 Hz/point, or 1.47 Hz/point following processing). From the Karplus relationship,[32,33] this is consistent with a dihedral angle of 180 °. Studies of other com-

pounds described in the literature also support this assertion. For example, Roush and co-workers report a coupling constant of 11.5 Hz for **15**, a rigid bicyclic structure used as an intermediate in their studies towards the total synthesis of FR182877.[34]

Table 2. NMR assignments and structure numbering for **5** (derived from the HSQC spectrum).

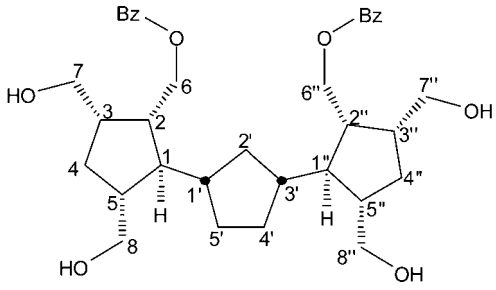

Position	^{13}C (ppm)	^{1}H (ppm)
1,1′′	50.6	1.52
2,2′′	44.8	2.3
3,3′′	45.4	2.2
4,4′′	34.3	2.2, 1.9
5,5′′	47.8	1.97
1′,3′	46.7	1.97
2′	38.7	2.15, 0.92
4′,5′	30.5	1.91, 1.27
6,6′′	67.0	4.28, 4.16
7,7′′	63.7	3.58, 3.70
8,8′′	67.5	3.58, 3.39

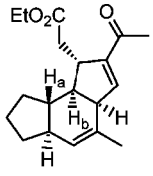

15, $^{3}J(H_a, H_b) = 11.5$ Hz

Peak volumes from the 300-ms NOESY spectrum were inspected in order to generate a set of strong (1.75 Å ± 0.75 Å), medium (3.00 Å ± 0.5 Å) and weak (4.25 ± 0.75 Å) distance restraints.[35] A total of 16 unique non-vicinal restraints were observed; accounting for symmetry, these translated into 32 unique distance restraints in the structure calculation (Figure 5). In assigning distance restraints, we made the assumption that where two possible assignments could be made for symmetry-related protons, geometric considerations would dictate that the restraint pair with the shorter apparent distance was more likely. For example, one could assign the NOE constraint from the symmetry-related pair of protons 5,5′′ to 3,3′′ as an inter-ring distance (Figure 6, a) or as an intra-ring restraint (Figure 6, b). While a conformation is conceivable that would allow for the inter-ring distance to be shorter than the intra-ring distance, this would preclude a 180° torsional angle for at least one of the 1,1′′–1′,3′ angles. Thus, the restraint was assigned as shown in Figure 6 (b). For diastereotopic proton pairs (those α to ester oxygen atoms, in this case), identical restraints were assigned to both protons. This represents an unfortunate degradation in the precision of the output conformational ensemble, because differences in NOE peak volumes are clearly visible for these proton pairs in the NOESY spectra. However, it was also unavoidable, because at this stage we are not able to individually assign these protons with confidence. NOE peaks are not observed between benzoate ring protons and the core *ter*-cyclopentane, indicating that these moieties are extended away from the core structure.

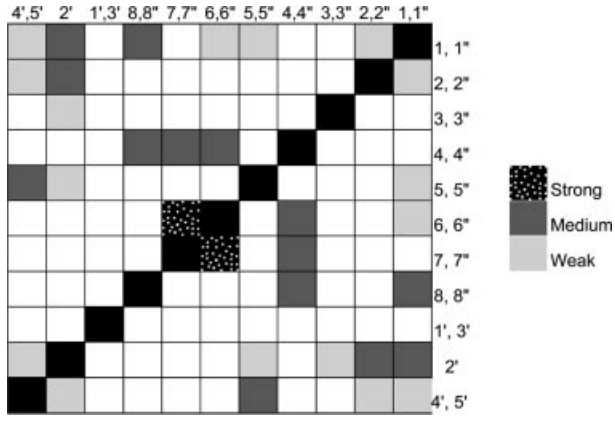

Figure 5. Distance restraints derived from the NOESY spectrum of **5** in CD_3OD.

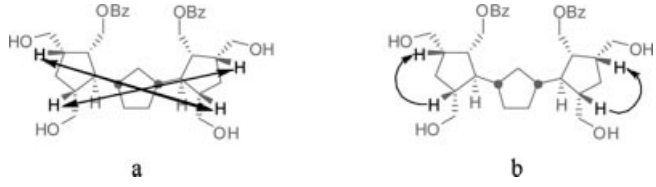

Figure 6. Hypothetical alternative NOE assignments for the 5,5′′–3,3′′ crosspeak.

Structure Calculations for 5

The 32 unique NOE distance restraints and the two inter-ring torsional restraints were used as the basis for restrained conformational analysis of **5**. The Monte–Carlo multiple minimum (MCMM) method implemented in Macromodel 7.2 was employed to generate 10,000 conformers. Structures were minimized using the Merck molecular mechanics force field (MMFFs) and the generalized Born/solvent accessible surface (GB/SA) continuum solvation model for water. While the similarity in rank ordering of dicyclopentane conformers for different force fields described above suggests that any of the commonly available force fields would suffice for our purposes, we chose to move forward with the MMFFs force field because of its reported high accuracy for conformational energies across a broad range of structural types.[36] Torsional bonds varied and ring closure bonds are indicated in Figure 7. Structures falling within a 50 kJ/mol (12.5 kcal/mol) energy window were retained, and rank-ordered according to energy. For comparison, identical conformation searches were performed without the torsional restraints, and without the

distance and torsional restraints. An analogous computational protocol has been applied by Smith and co-workers in the analysis of a β-turn peptidomimetic[37] and (+)-discodermolide,[38] and by Paterson and co-workers towards the solution structural determination of laulimalide.[39]

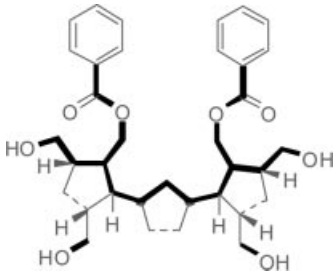

Figure 7. Torsional bonds varied (black lines) and ring closures (dotted lines) in restrained and unrestrained conformational analysis of **5**.

Results

Figure 8 shows an overlay of the 10 lowest energy output structures from the conformational analysis of **5** without, with distance, and with distance and torsional NMR-derived restraints. Incorporation of NMR distance restraints clearly reduces the conformational degrees of freedom falling within the designated potential energy window, although the lack of observed NOEs to benzoate side chains means the position of these groups is not precisely defined. None of the low-energy structures were found to have any NOE violations. As expected, application of the strong dihedral angle restraint to the inter-ring torsion results in all of the output structures of **5** adopting the *anti*/*anti* inter-ring geometry. Additionally, the incorporation of this torsional restraint to the distance restrained analysis greatly enhances the convergence of conformations occupying the potential energy window. This is in excellent qualitative agreement with the lowest-energy structure obtained by unrestrained conformational analysis. The lowest energy

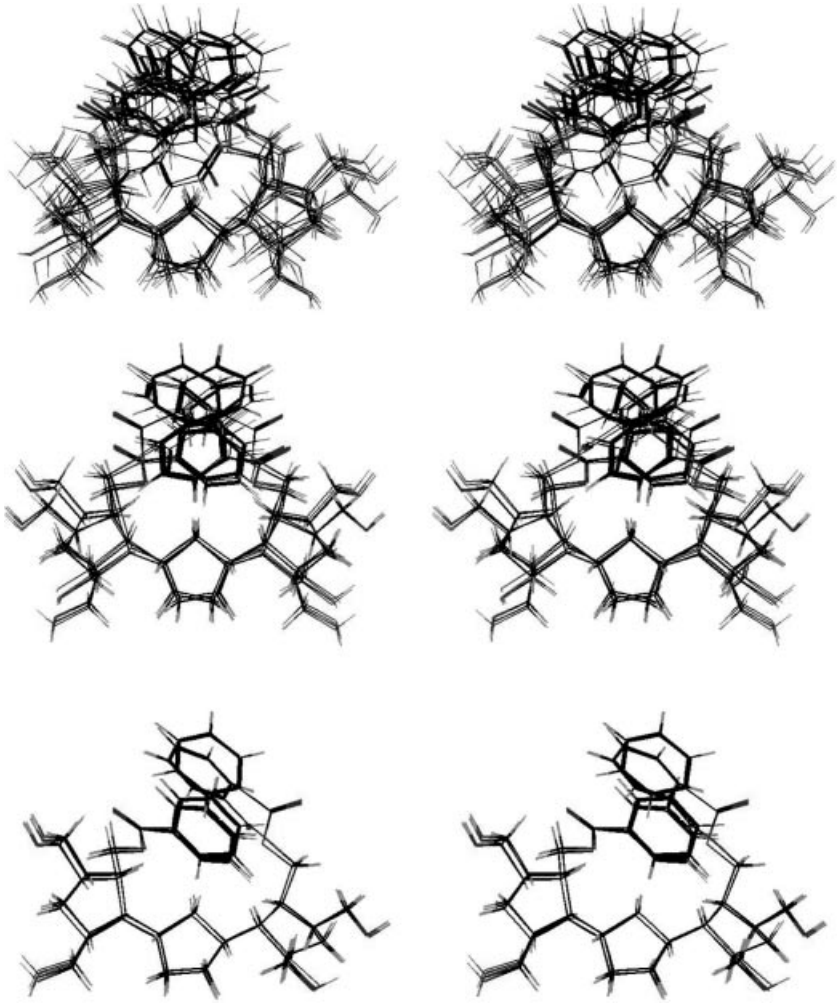

Figure 8. Wall-eyed stereoview of the overlay of the first 10 lowest energy output structures from conformation searches (MCMM, MMFFs, GB/SA H_2O) for **5** in the absence of NMR-derived restraints (top, lowest 0.4 kcal/mol of output structures), in the presence of only NMR-derived distance restraints (middle, lowest 1.4 kcal/mol of output structures), and in the presences of both NMR-derived distance and torsional restraints (bottom, lowest 3.0 kcal/mol of output structures). This figure was generated with Maestro.[14]

NMR-derived structure features a central cyclopentane in the envelope conformation, with the two substituent cyclopentanes in a pseudoequatorial orientation.

Conclusions

While determination of a single lowest-energy conformation by NMR is complicated by solution phase dynamics, detailed structural information about low energy conformations is readily obtainable. In this study, comparison of the ensemble of the 10 lowest energy structures, in addition to the highest and lowest energy conformers, reveals the rigid behavior of the core *ter*-cyclopentane scaffold in solution. As we have demonstrated elsewhere, the *ter*-cyclopentane scaffold has promise as a new structural motif for molecular recognition and biosensing. The experimental and computational analysis presented here serves to confirm our initial hypotheses regarding the likely solution conformation of *cis* 1,3-*ter*-cyclopentanes as rigid easily derivatizable molecular recognition scaffolds, with significant agreement between conformational analyses with and without application of experimentally derived distance and torsional restraints. The work described herein proves the utility of *ter*-cyclopentanes as molecular recognition scaffolds, and provides a foundation for moving forward with additional structural studies.

Experimental Section

General Experimental Details: All nonaqueous reactions were conducted in flame-dried glassware under N_2, and were stirred with a teflon-coated magnetic stir bar, unless otherwise stated. Air-sensitive reagents and solutions were transferred through syringe (unless otherwise stated) and were introduced to the reaction vessel through a rubber septum. Room temperature (r.t.) refers to ambient temperature, which is approximately 22 °C. Unless otherwise stated, temperatures other than r.t. denote the temperature of the cooling/heating bath. All distillations were performed under N_2, or at reduced pressure using a water aspirator (15–30 Torr), or vacuum pump (1 Torr).

Reagent-grade solvents were used without further purification for all extractions and work-up procedures. Double distilled water was used for all aqueous reactions, work-ups, and for the preparation of all aqueous solutions. Reaction solvents were dried and purified according to standard procedures by distillation under N_2 from an appropriate drying agent, or by purification through a Glas-Col solvent drying system. Cyclopentadiene was cracked at 140 °C, and stored indefinitely at –80 °C.

Proton NMR spectra were obtained with a Bruker Avance 400 (400 MHz), Avance 500 (500 MHz) or a Varian Inova-500 (500 MHz) instrument at 25 °C. Carbon NMR spectra were acquired with an Avance 400 (101 MHz), or with a Varian Inova-500 (126 MHz). Chemical shifts are reported in ppm (δ) relative to the appropriate deuterated solvent. Infrared (IR) spectra were recorded with a Perkin–Elmer 1610 FT-IR spectrophotometer and are reported in wavenumbers (cm^{-1}) with a polystyrene standard. High resolution mass spectrometry (HRMS) was performed at the national mass spectrometry facility at the University of California, Riverside, California.

Cyclopentane-1,3-dicarbaldehyde (9): Norbornene (5.0 g) was dissolved in 170 mL CH_2Cl_2 in a 250-mL round-bottom flask. $KMnO_4$ (54 g) and $CuSO_4{\cdot}5H_2O$ (27 g) was ground to a fine powder using a mortar and pestle. This fine powder (76 g) was placed in a 1000-mL round-bottom flask equipped with an overhead stirrer. H_2O (2.5 mL) and CH_2Cl_2 (100 mL) were added, and stirring was started. After 5 min, the solution of norbornene in CH_2Cl_2 was added. After an additional 10 min of stirring, *t*BuOH (12 mL) was added, and this mixture stirred for 12 h at room temperature. At this point, TLC of the reaction mixture showed complete consumption of starting material. The slurry was filtered through Celite, dried with Na_2SO_4, filtered, and reduced in vacuo. Because of the volatility of the compound, care must be taken at this stage to prevent product loss. Compound **9** was obtained in essentially quantitative yield, and exhibited spectral characteristics identical to literature reports.

Bis-α,β-unsaturated Ester 11: The Phenethyl diisopropyl phosphonate **10** (62.8 g, 191.4 mmol) was dissolved to a concentration of 0.5 M in THF at 0 °C, and allowed to stand at that temperature 30 min to ensure thermal equilibration. Addition of potassium *tert*-butoxide (20.06 g, 178.78 mmol) to the phosphonate solution resulted in a canary yellow reaction color. After stirring for 20 min at 0 °C, or until the entire base had dissolved in the reaction mixture, the reaction was warmed to room temp. and stirred for an additional 2 h. Concurrently, the aldehyde **9** (10.72 g, 85.1 mmol) was dissolved into 2.0 M THF, and cooled to –78 °C for 30 min. The yellow potassium anion of **10** was added by a cannula to the aldehyde solution over 1.5 h. After addition of the anion was complete, the reaction was maintained at –78 °C for 10 h with monitoring by TLC. The reaction was quenched with water (400 mL), and the resulting layers were separated. The aqueous layer was extracted with diethyl ether (4 × 250 mL). The organics were pooled and washed with a brine solution, dried with Na_2SO_4, filtered, and reduced in vacuo to give a yellow oil. Purification of the yellow residue by flash chromatography (silica, 80:20 to 60:40 hexanes/diethyl ether) afforded **11** as a pale yellow oil (21.7 g, 61% yield, *E*,*E*:*E*,*Z* >20:1).

Compound 11: ^{1}H NMR (400 MHz, $CDCl_3$): δ = 7.32–7.35 (m, 4 H), 7.24–7.27 (m, 6 H), 6.93 (apparent dd, $^3J_{H,H}$ = 8, 16 Hz, 2 H), 5.80 (apparent dd, $^3J_{H,H}$ = 1, 16 Hz, 2 H), 4.37 (t, $^3J_{H,H}$ = 7 Hz, 4 H), 3.0 (t, $^3J_{H,H}$ = 7 Hz, 4 H), 2.71–2.82 (m, 2 H), 2.04–2.10 (m, 1 H), 1.91–2.01 (m, 1 H), 1.76 (t, $^3J_{H,H}$ = 8 Hz, 1 H), 1.37–1.62 (m, 2 H), 1.29–1.37 (m, 1 H) ppm. ^{13}C NMR (75 MHz, $CDCl_3$): δ = 166.5, 155.5, 152.2, 137.8, 128.8, 128.4, 126.5, 119.7, 119.6, 64.7, 42.6, 41.3, 38.9, 37.6, 35.1, 32.1, 31.1 ppm. FTIR (thin film, from $CDCl_3$): $\tilde{\nu}$ = 3060, 3026, 2951, 1714, 1650, 1496, 1453, 1149, 984 cm^{-1}. HRMS Calculated for $C_{27}H_{31}O_4$ [M + H] 419.2222; found 419.2224.

Diels–Alder Adduct 12: Dienophile **11** (20 g, 47.7 mmol) was dissolved to a concentration of 0.3 M in CH_2Cl_2. The resulting solution was cooled to 0 °C for 15 min. Addition of Me_3Al (1.19 mL, 2.39 mmol, 2.0 M in hexanes) yielded slight gas evolution, which dissipated upon stirring at 0 °C for an additional 10 min. To the yellow solution was added $AlCl_3$ (23.8 mL, 23.85 mmol, 1.0 M in CH_3NO_2) and the reaction was stirred an additional 5 min at 0 °C. Cyclopentadiene (31.4 g, 477 mmol, 4.0 M in CH_2Cl_2) was added to the colorless solution by an addition funnel dropwise over 30 min. The reaction was warmed to 4 °C, and allowed to stir at 4 °C for 12 h. The reaction was quenched with pyridine (20 mL), the reaction was quickly warmed to room temp. The resulting thick white slurry was filtered through silica (300 mL), and washed with Et_2O (5 × 100 mL). The organics were reduced in vacuo. Azeotropic re-

moval of the pyridine and CH_3NO_2 was accomplished by treatment with heptane (4 × 50 mL) and rotary evaporation, affording a yellow residue. Purification by flash chromatography (silica, 95:5, hexanes/Et_2O) afforded a mixture of the *endo–endo* convex–convex and convex–concave/concave–convex diastereomers of the cycloadduct **12** in 70% yield. The mixture was brought up in DMSO (0.1 parts), then diluted with CH_3OH (3 parts) and CH_3CN (1 part). The convex–convex diastereomer was separated in 15% yield by reverse phase (C_{18}) preparatory HPLC with a 92% CH_3CN, 8% H_2O, 0.1% TFA isocratic method with approximately a 15% yield of the desired convex-convex product.

Compound 12: ^{1}H NMR (400 MHz $CDCl_3$): δ = 7.35–7.22 (m, 10 H), 6.26–6.24 (m, 2 H), 5.87–5.84 (m, 2 H) 4.27–4.14 (m, 4 H), 3.09 (s, 2 H) 2.93–2.89 (t, $^3J_{H,H}$ = 6 Hz, 3 H), 2.67 (s, 2 H) 2.54–2.52 (t, $^3J_{H,H}$ = 4 Hz, 2 H), 1.94–1.88 (m, 3 H), 1.76–1.70 (m, 2 H), 1.63–1.59 (m, 2 H), 1.54 (s, 1 H), 1.52 (s, 1 H), 1.43–1.34 (m, 5 H), 1.13–1.06 (q, $^3J_{H,H}$ = 12 Hz, 1 H) ppm. ^{13}C NMR (75 MHz $CDCl_3$): δ = 30.7, 34.9, 38.8, 45.6, 46.1, 46.3, 46.4, 49.4, 50.0, 64.6, 126.4, 128.4, 128.9, 133.3, 137.9, 138.5, 174.5 ppm. FTIR (thin film, from $CDCl_3$): $\tilde{\nu}$ = 3061, 3026, 2940, 2867, 1731, 1454, 1331, 1261, 1167, 1116, 1015, 698 (cm^{-1}). HRMS Calculated for $C_{37}H_{43}O_4$ [M + H] 551.3161 found 551.3177.

Reduction of 12 to 13: $LiAlH_4$ (79.8 mg, 2.1 mmol) was added to **12** (116 mg, 0.21 mmol) in 2 mL THF, at room temp. with slight gas evolution. The reaction stirred for 24 h at room temp., then was quenched sequentially with water (0.5 mL) and 10% NaOH aq. solution (0.5 mL), and diluted with 10 mL THF. The reaction formed a white precipitate and was stirred for 2 h at room temp. The reaction contents were filtered through Celite (400 mL), and the pad was washed with diethyl ether (5 × 100 mL). The filtrate was dried with Na_2SO_4, filtered and reduced in vacuo to give a yellow oil. Purification of the oil by flash chromatography (silica, 66:34 hexanes/ethyl acetate) afforded the diol (34 mg, 51% yield).

Compound 13: ^{1}H NMR (400 MHz $CDCl_3$): δ = 6.17 (s, 2 H), 6.02 (s, 2 H), 3.52–3.47 (m, 2 H), 3.14 (t, $^3J_{H,H}$ = 10 Hz, 2 H), 2.90 (s, 2 H), 2.56 (s, 2 H), 1.87 (d, $^3J_{H,H}$ = 6 Hz, 4 H), 1.73–1.70 (m, 5 H), 1.48–1.40, (m, 5 H), 1.25–1.19 (m, 6 H), 0.741 (q, $^3J_{H,H}$ = 12 Hz, 1 H), 0.56 (m, 2 H) ppm. ^{13}C NMR (75 MHz $CDCl_3$): δ = 30.9, 39.9, 43.7, 45.7, 46.0, 46.1, 48.6, 49.1, 66.5, 133.2, 138.1 ppm. FTIR (thin film, from $CDCl_3$): $\tilde{\nu}$ = 3213, 2960, 2360, 1012, 725 cm^{-1}. HRMS Calculated for $C_{21}H_{31}O_2$ [M + H] 315.2324 found 315.2316.

Di-benzoate 14: The di-alcohol derived from reduction of **13** (34 mg, 0.11 mmol) was slurried into CH_2Cl_2 at room temp. to provide a 0.2 M solution. Sequential addition of benzoyl chloride (55 mg, 0.38 mmol), and Et_3N (0.06 mL, 0.432 mmol) at room temp. to the slurry caused the reaction to become yellow and homogeneous. After stirring for 24 h at room temp. TLC analysis showed consumption of starting material. The reaction was quenched with water (0.5 mL), and dried to yield a white solid. Purification of the oil by flash chromatography (silica, 95:5 hexanes/diethyl ether) yielded **14** (15 mg, 18% yield) as a colorless oil.

Compound 14: ^{1}H NMR (400 MHz $CDCl_3$): δ = 8.03–8.01 (m, 4 H), 7.52 (t, $^3J_{H,H}$ = 8 Hz, 2 H), 7.39 (t, $^3J_{H,H}$ = 8 Hz, 4 H), 6.24–6.22 (m, 2 H), 6.05–6.03 (m, 2 H), 4.2 (apparent d of d, $^3J_{H,H}$ = 4.8 Hz, $^3J_{H,H}$ = 6.4 Hz, 4 H), 3.77 (t, $^3J_{H,H}$ = 10 Hz, 2 H), 2.92 (s, 2 H), 2.60 (s, 2 H) 2.26–2.12 (m, 3 H), 1.94–1.88 (m, 2 H), 1.82–1.75 (m, 2 H), 1.55 (s, 1 H), 1.51–1.41 (m, 4 H), 1.31–1.25 (m, 7 H), 0.92–0.82 (m, 3 H) 0.74 (apparent d of d, $^3J_{H,H}$ = 4 Hz, $^3J_{H,H}$ = 10 Hz, 2 H) ppm. ^{13}C NMR (75 MHz, $CDCl_3$): δ = 166.4, 138.3, 133.5, 132.6, 129.6, 128.2, 68.2, 49.2, 46.2, 46.0, 45.8, 45.0, 44.2, 39.7, 30.9, 30.7 ppm. FTIR (thin film, from $CDCl_3$): $\tilde{\nu}$ = 2963, 1717, 1451, 1313, 1271, 1175, 1110, 1069, 1026, 710 cm^{-1}. HRMS Calculated for $C_{35}H_{38}O_4$ (M+) 522.2770; found 522.2752.

Tetra-Alcohol 5: The di-benzoate **14** (15 mg, 0.028 mmol) was dissolved to a concentration of 0.1 M in a solution of 1:1 CH_2Cl_2/MeOH, and cooled to –78 °C for 10 min. Next, O_3 was bubbled through the solution, until the reaction mixture became deep blue in color (10 min). O_3 treatment was continued for an additional 35 min. O_3 bubbling was then discontinued, and began bubbling O_2, to remove excess O_3. Once the blue color dissipated, the reaction was warmed to 0 °C for 10 min. $NaBH_4$ (14.8 g, 0.402 mmol) was added yielding slight gas evolution and the vessel was allowed to slowly warm to room temp. over 30 min. The reaction was stirred for 4 h at room temp. then quenched with 10% aq. HCl (0.4 mL). The contents were diluted with ethyl acetate, and the layers were separated. The aqueous layer was extracted with ethyl acetate (4 × 1 mL). The organic extracts were combined and washed sequentially with water (1 mL), satd. aq. Na_2CO_3 (1 mL), and satd. aq. NaCl (1 mL). The organics were dried with Na_2SO_4, filtered, and reduced in vacuo to afford an opaque solid **5** (15 mg, 89% yield) as a clear oil.

Compound 5: ^{1}H NMR (400 MHz CD_3OD): δ = 7.96 (d, $^3J_{H,H}$ = 6.8 Hz, 4 H), 7.53–7.51 (m, 2 H), 7.42 (t, $^3J_{H,H}$ = 8 Hz, 4 H), 4.30–4.26 (m, 2 H), 4.18–4.14 (m, 2 H), 3.71–3.69 (m, 2 H) 3.63–3.58 (m, 4 H), 3.39 (m, 2 H) 2.34–2.23 (m, 4 H), 1.98–1.95 (m, 7 H), 1.77–1.74 (m, 2 H), 1.53 (t, $^3J_{H,H}$ = 6 Hz, 2 H), 1.36–1.26 (m, 7 H), 0.94–0.86 (m, 2 H) ppm. ^{13}C NMR (75 MHz CD_3OD): δ = 168.2, 134.2, 131.6, 130.6, 129.6, 67.5, 67.0, 63.7, 50.6, 47.8, 46.7, 45.4, 44.8, 38.7, 34.3, 30.5 ppm. FTIR (thin film, from CD_3OD): $\tilde{\nu}$ = 3323, 2923, 2361, 1716, 1450, 1276, 1114, 1070, 1026, 712 cm^{-1}. HRMS Calculated for $C_{35}H_{47}O_8$ [M + H] 595.3270 found 595.3263.

Experimental Procedures for 2D NMR Sample Preparation and Data Acquisition: The tetra-alcohol **5** (15 mg, 0.025 mmol) was dissolved into 0.3 mL of CD_3OD, that had been dried by treating with 4-Å molecular sieves, to afford a 8.3 mM solution. The solution was transferred to an NMR tube, under N_2. N_2 was bubbled through the solution for 10 min, to remove dissolved O_2. All 2D NMR experiments were performed with a Bruker Avance-500. A constant temperature of 25 °C was used for all experiments. DQF-COSY spectra were acquired with a sweep width of 12.0 ppm in both dimensions, and a digital resolution of 2.9 Hz/point in F2 and 11.7 Hz/point in F1. Zerofilling in both dimensions during processing provided a final digital resolution of 1.47 Hz/point. NOESY spectra were acquired using a sweep width of 10.00 ppm in each dimension, and a mixing time of 300 ms. HSQC spectra were acquired with sweep widths of 10 ppm in *F*2 (^{1}H) and 220 ppm in *F*1 (^{13}C). Data processing was performed using MestReC[40] on a Windows PC, with 90 degree sinebell-squared apodization functions applied in each dimension during processing.

Supporting Information (see also the footnote on the first page of this article): Spectral information and all 2D NMR experiments (21 pages).

Acknowledgments

Funding by NIH-NIGMS (R01-GM-062825-03) and DHHS-PHS (2T32AR007472-16) is gratefully acknowledged.

[1] F. R. Jensen, C. H. Bushweller, *J. Am. Chem. Soc.* **1969**, *91*, 5774.
[2] M. T. Burger, A. Armstrong, F. Guarnieri, D. Q. McDonald, W. C. Still, *J. Am. Chem. Soc.* **1994**, *116*, 3593–3594.

[3] T. Brandl, R. W. Hoffmann, *Eur. J. Org. Chem.* **2004**, 4373–4378.
[4] T. Trieselmann, R. W. Hoffmann, K. Menzel, *Eur. J. Org. Chem.* **2002**, 1292–1304.
[5] A subset of work in this area includes: a) R. E. Taylor, Y. Chen, G. M. Galvin, P. K. Pappa, *Org. Biomol. Chem.* **2004**, *2*, 127–132.
[6] H. B. Lee, M. C. Zaccaro, M. Pattarawarapan, S. Roy, H. U. Saragovi, K. Burgess, *J. Org. Chem.* **2004**, *69*, 701–713.
[7] J. D. Sadowsky, M. A. Schmitt, H.-S. Lee, N. Umezawa, S. Wang, Y. Tomita, S. H. Gellman, *J. Am. Chem. Soc.* **2005**, *127*, 11966–11968.
[8] For an early synthesis of the parent *ter*-cyclopentane hydrocarbon, see:J. v. Braun, J. Reitz-Kopp, *Ber. Dtsch. Chem. Ges.* **1941**, *74*, 1105–1110.
[9] A more recent synthesis of polycyclohexylcyclohexanes may be found in: I. Columbus, R. E. Hoffman, S. E. Biali, *J. Am. Chem. Soc.* **1996**, *118*, 6890–6896.
[10] M. Yoshida, M. Ezaki, M. Hashimoto, M. Yamashita, N. Shigematsu, H. Okuhara, M. Kohsaka, K. Horikoshi, *J. Antibiot.* **1990**, *43*, 748.
[11] M. S. Kuo, R. J. Zielinski, J. I. Cialdella, C. K. Marschke, M. J. Dupuis, G. P. Li, D. A. Kloosterman, C. H. Spilman, V. P. Marshall, *J. Am. Chem. Soc.* **1995**, *117*, 10629.
[12] For lead references, see: J. Pietruszka, *Chem. Rev.* **2003**, *103*, 1051–1070.
[13] R. D. Hubbard, S. R. Horner, B. L. Miller, *J. Am. Chem. Soc.* **2001**, *123*, 5810–5811.
[14] C. R. H. Raetz, *Annu. Rev. Biochem.* **1990**, *59*, 129–170.
[15] D. C. Morrison, D. M. Jacobs, *Immunochemistry* **1976**, *13*, 813–818.
[16] S. Chan, S. R. Horner, B. L. Miller, P. M. Fauchet, *J. Am. Chem. Soc.* **2001**, *123*, 11797–11798.
[17] U. Burkert, N. L. Allinger, "Molecular Mechanics" (ACS Monograph 177), American Chemical Society, Washington, D. C., **1982**, p. 87.
[18] W. Ritter, W. Hull, H.-J. Cantow, *Tetrahedron Lett.* **1978**, *19*, 3093.
[19] D. H. Wertz, N. L. Allinger, *Tetrahedron* **1974**, *30*, 1579.
[20] L. Lunazzi, D. Macciantelli, F. Bernardi, K. U. Ingold, *J. Am. Chem. Soc.* **1977**, *99*, 4573.
[21] R. H. Boyd, *J. Am. Chem. Soc.* **1975**, *97*, 5353.
[22] Macromodel 7.2; Schroedinger, Inc.
[23] W. C. Still, A. Tempczyk, R. C. Hawley, T. Hendrickson, *J. Am. Chem. Soc.* **1990**, *112*, 6127.
[24] J. E. Kilpatrick, K. S. Pitzer, R. Spitzer, *J. Am. Chem. Soc.* **1947**, *69*, 2483–2488.
[25] F. V. Brutche Jr., T. Roberts, S. J. Barr, N. Pearson, *J. Am. Chem. Soc.* **1959**, *81*, 4915–4920.
[26] F. V. Brutcher Jr., W. Bauer Jr., *J. Am. Chem. Soc.* **1962**, *84*, 2233–2236.
[27] D. G. Lee, T. Chen, Z. Wang, *J. Org. Chem.* **1993**, *58*, 2918–2919.
[28] H. Becker, M. A. Soler, K. B. Sharpless, *Tetrahedron* **1995**, *51*, 1345–1376.
[29] S. Göksu, R. Altundas, Y. Sütbeyaz, *Synth. Commun.* **2000**, *30*, 1615.
[30] R. D. Hubbard, B. L. Miller, *J. Org. Chem.* **1998**, *63*, 4143.
[31] H. Nagaoka, Y. Kishi, *Tetrahedron* **1981**, *37*, 3873–3888.
[32] M. Karplus, *J. Am. Chem. Soc.* **1963**, *85*, 2870.
[33] C. A. G. Hassnoot, F. A. A. M. De Leeuw, C. Altona, *Tetrahedron* **1980**, *36*, 2783.
[34] J. L. Methot, W. R. Roush, *Org. Lett.* **2003**, *5*, 4223–4226.
[35] M. Williamson, T. Havel, K. Wüthrich, *J. Mol. Biol.* **1985**, *182*, 295–315.
[36] T. A. Halgren, *J. Comput. Chem.* **1999**, *20*, 730–748.
[37] A. B. Smith III, W. Wang, P. A. Sprengeler, R. Hirschmann, *J. Am. Chem. Soc.* **2000**, *122*, 11037–11038.
[38] A. B. Smith III, M. J. LaMarche, M. Falcone-Hindley, *Org. Lett.* **2001**, *3*, 695–698.
[39] I. Paterson, D. Menche, R. Britton, A. E. Håkansson, M. A. Silva-Martínez, *Tetrahedron Lett.* **2005**, *46*, 3677–3682.
[40] MestReC, Mestrelab Research Company, http://www.mestrec.co.

Received: September 15, 2006
Published Online: November 13, 2006

